

Real time evolution in spin diffusion on magnetic cluster

R. Lahreche¹, R.-J. Tarento^{2,a}, P. Joyes², J. van de Walle², and D.E. Mekki¹

¹ Faculté des Sciences, Département de Physique, Université d'Annaba, B.P. 12, Annaba, Algeria

² Laboratoire de Physique des Solides, bâtiment 510, Université d'Orsay, 91405 Orsay Cedex, France

Received 10 September 2002

Published online 3 July 2003 – © EDP Sciences, Società Italiana di Fisica, Springer-Verlag 2003

Abstract. We investigate the diffusion of a spin polarized projectile on a ferromagnetic spin polarized cluster. The interaction between the projectile and the target is described with a Heisenberg Hamiltonian which excludes the charge degree of freedom during the process. Our calculation is based on a real time description of the spins of the two interacting systems. We deduce from it the depolarization cross-section of the projectile and the excitation in the cluster *versus* its size, the impact parameter and the kinetic energy. We analyze 3 different behaviors of the system according to whether the intra-cluster excitations propagate slower or faster than the projectile.

PACS. 36.40.-c Atomic and molecular clusters – 36.40.Cg Electronic and magnetic properties of clusters

1 Introduction

In the last years, a lot of papers have been devoted to the experimental study of the interaction between a fast atomic particle with a metallic cluster. If we limit ourselves to collisions without fragmentation, various kinds of non-adiabatic effects have been observed such as electronic excitation, ionization and capture [1]. Theoretical papers on these various phenomena have been published [2].

Other experiments have been performed on the spin diffusion on magnetic targets. Let us mention the formation of spin-polarized electrons in collisions of multicharged ions with a magnetized iron surface [3] and the spin depolarization of low energy polarized electrons through ferromagnetic films [4]. Though, up to now, only bulk targets are employed, similar experiments could be made in the next future on finite media or aggregates. In this paper we intend to develop a theoretical description of this kind of phenomenon.

We will use a time dependent Heisenberg formalism which will be presented in Section 2. In Section 3 we discuss our results on the spin diffusion on cluster.

2 The Heisenberg Hamiltonian

The Heisenberg Hamiltonian has been widely used in solid state physics, it has also been employed for aggregates, in particular to investigate the π electron magnetic properties in polyenes [5]. It can be written

$$H^{Heis} = - \sum_{i,j} J_{ij} \mathbf{S}_i \mathbf{S}_j \quad (1)$$

where in the present study of a spin diffusion on a spin polarized system, one of the sites, say site 1, is moving along a given trajectory while the target sites are assumed fixed. Between two nearest target atoms the J_{ij} interaction term is constant and worth J_o . The dependence of J_{i1} or J_{1i} on the r_{1i} distance between the target atom i and the incident atom 1 can be taken as:

$$J_{i1} = J_{1i} = J'_o \exp\left(-\frac{r_{1i}}{r_o}\right) \quad (2)$$

J'_o has been chosen in our calculation such that, when r_{1i} is equal to the nearest target distance, J_{i1} is equal to J_o . $r_o \cong 1 \text{ \AA}$ is a typical interaction length. The various r_{1i} distances between the incident and the target particles depend on time t . We will assume that in the studied speed range, the particle 1 motion does not depend on the spin evolution during the interaction. We will only consider linear trajectories with constant velocities v_o .

The model assumes localized spins and neglects any charge excitations during the dynamics *i.e.*: both modification of the electronic configuration inside the cluster and charge transfer between the projectile and the cluster leading to a charge capture at large projectile velocity. For large intrasite electronic correlation, such charge excitations are not important and hence the Heisenberg model seems to be justified and could be applied to large cluster (*i.e.*: several hundred atoms).

3 Results of the Heisenberg model for small aggregates

We consider the collision of an up incident spin on a ferromagnetic down spin target both initially polarized along

^a e-mail: tarento@lps.u-psud.fr

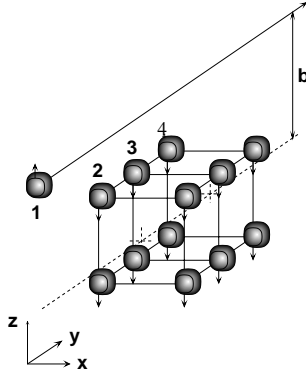


Fig. 1. Geometry and initial spin configuration for a spin diffusion on a cluster C_2 .

the z -axis. Therefore we take a $J_o = 0.1$ eV positive value so that the initial target spin configuration is the ground state. The target, called C_n is a linear assembly of n cubes along the y -axis, the number of sites is $4(n+1)$ and the nearest neighbor distance is 2 \AA . The projection on the y -axis of the C_n sites are $2, 4, \dots, 2(n+1) \text{ \AA}$. The trajectory is contained in a plane parallel to Oyz plane at a distance b from the aggregate axis (Fig. 1).

The wave function $|\Phi\rangle$ is written as:

$$|\Phi\rangle = \sum_i \alpha_i |\phi_i\rangle \quad (3)$$

$\{|\phi_i\rangle\}$ are the states $|\uparrow; \downarrow, \dots, \downarrow\rangle, |\downarrow; \uparrow, \downarrow, \dots, \downarrow\rangle \dots$ with only one up spin for the projectile and cluster system (the first spin is referred to the projectile one). The time dependence of the coefficients α_i are obtained by solving numerically the Schrödinger equation with for the initial configuration $|\uparrow; \downarrow, \dots, \downarrow\rangle$. At every time of the dynamics the conservation of the total spin S_z and S^2 of the projectile and cluster has been checked.

In Figure 2, we give $S_z^i(Y)$ for $b = 4 \text{ \AA}$ and different velocities: $v_o = 1.88 \times 10^5 \text{ m/s}$ ($E^{\text{Ag}} = 20 \text{ keV}$) in Figures 2a and 2b; $v_o = 0.597 \times 10^5 \text{ m/s}$ ($E^{\text{Ag}} = 2 \text{ keV}$) in Figures 2c and 2d and $v_o = 0.26 \times 10^5 \text{ m/s}$ ($E^{\text{Ag}} = 0.4 \text{ keV}$) in Figures 2e and 2f.

For discussing these results we need two characteristic times $\tau = \hbar/J_o = 4.6 \times 10^{-14} \text{ s}$ which describes intra atomic cluster spin propagation and $\tau'(v_o)$ the travelling time along one atomic distance.

In Figures 2a and 2b, $\tau' = 1.65 \times 10^{-14} \text{ s} < \tau$. We observe that the S_z^i target spins begin to vary significantly when the incident spin is just above them. There is a decrease of the spin change from $i = 2$ to 4. These results can be physically understood. Due to the relatively small τ' time each site behave as if it were isolated. The amplitude decrease is due to the incident spin decrease.

It may be noticed that an exact solution of a two-spin Hamiltonian

$$H = J_{12} \mathbf{S}_1 \mathbf{S}_2 \quad (4)$$

with $J_{12} = J_o \exp(-\eta t)$ and $\eta = v/r_o$ confirms the interpretation. If, at time $t = 0$, the system is in the antiparallel groundstate (up and down on sites 1 and 2) the weight

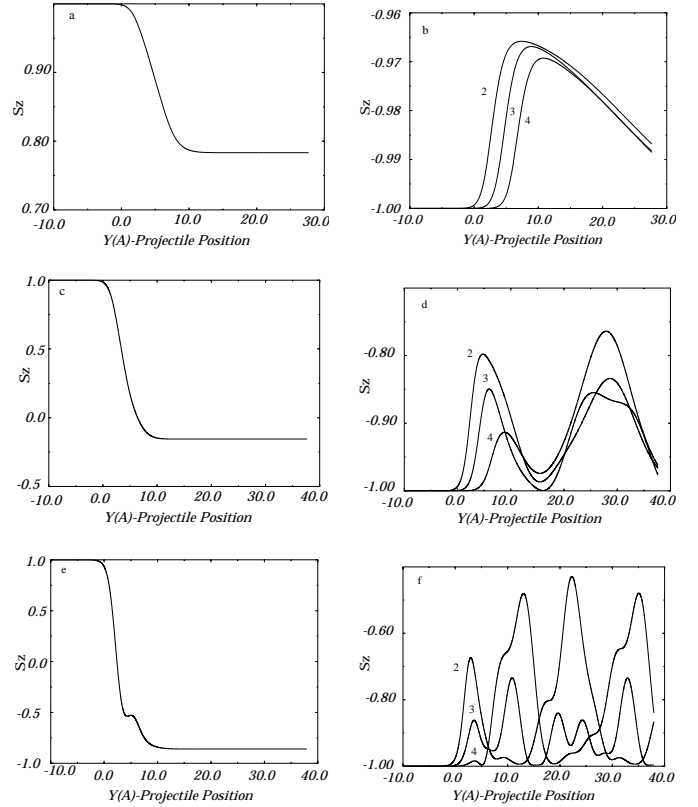


Fig. 2. Evolution of the z spin component S_z for the projectile (cluster C_2 atoms) in (a, c, e) and (b, d, f) versus different projectile velocity v_o . Y is the projectile position for a trajectory parallel to the C_2 axis in the median plane versus a face with an impact parameter $b = 4 \text{ \AA}$. The initial spin state and the studied target atoms (2-4) are reported in Figure 1.

on this spin configuration decreases with time (or with Y traveled by atom 1) as $\cos^2(2\alpha(t))$ with

$$\alpha(t) = \frac{J_o \hbar}{4\eta} (1 - \exp(-\eta t)).$$

By replacing the J_o and η values in this formula gives the behavior observed in Figures 2a (2b) in the vicinity of the first maxima.

In Figures 2c and 2d $\tau' = 3.35 \times 10^{-14} \text{ s}$ is of the order of the intra cluster time. We observe a main difference from the previous case. The S_z^1 (incident) and S_z^2, S_z^3, S_z^4 (target) initial amplitudes of variation are larger. This is due to a larger incident-site interaction which makes it more efficient. This effect is smaller for S_z^4 because the incident spin is almost completely flipped when it interacts with site 4.

As the velocity is still reduced (Figs. 2e and 2f, $\tau' = 7.5 \times 10^{-14} \text{ s}$) the incident spin flips almost completely. The target spins has a complex evolution. It is no longer possible to separate the incident and the intra-target effects. The incident spin interacts with a target having all its spin varying.

We give the results for the same velocity as in Figures 2a and 2b $v_o = 1.88 \times 10^5 \text{ m/s}$ and a trajectory

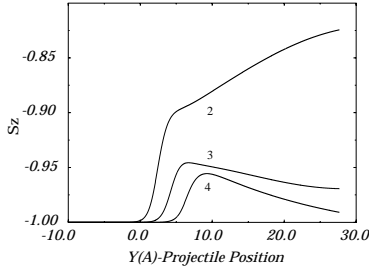


Fig. 3. Evolution of the z spin component S_z of the C_2 atoms (2-4). Y is the projectile position for a trajectory parallel to the C_2 axis in the median plane *versus* a face with an impact parameter $b = 0 \text{ \AA}$. The initial spin state and the studied target atoms (2-4) are reported in Figure 1.

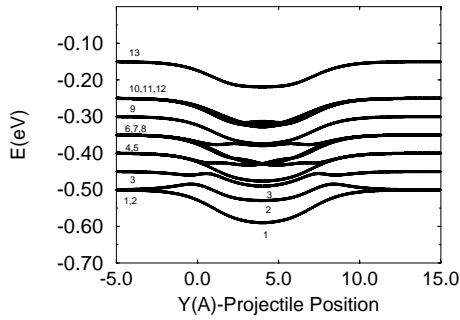


Fig. 4. The 13 adiabatic energy surfaces obtained by diagonalizing H^{Heis} note that when the projectile is far from the cluster some levels are degenerate but the degeneracy is removed during the collision. The surfaces are labeled from 1 to 13 *i.e.* from the lowest to highest energy surfaces.

along the molecule axis ($b = 0 \text{ \AA}$). There is no significant change for the incident spin. However the target spins behave differently (Fig. 3). In particular we see that now the S_z^2 up character is always increasing. This is due to the fact that the up character received from the incident spin is not reduced by sharing it with the 3 sites of the first square which have also received the same up character from the incident particle. It is even reinforced when the second square sites receive some up character and transfer it. Let us give some insights on the dynamics by introducing the 13 adiabatic surfaces obtained by diagonalizing H^{Heis} for the trajectory conditions of Figure 2 (see Fig. 4). These adiabatic surfaces are independent of the projectile speed and have an even symmetry with respect to the axis $Y = 4 \text{ \AA}$. When the projectile is far from the cluster some degeneracies are occurring. Only 7 energies levels (-0.5 eV , -0.45 eV , -0.4 eV , -0.35 eV , -0.30 eV , -0.25 eV and -0.15 eV) are possible. During the collision the degeneracies are removed. The adiabatic surfaces are labeled from 1 to 13 from the lowest energy surface to the highest one. To these adiabatic surfaces, time dependent states are associated which are expanded on the $|\phi_i\rangle$. Let us make some comments on the surfaces 1 and 2. They are degenerate when the projectile is far. Thus there is an arbitrary to choose these states but one possible choice could be the following: one state is $|a\rangle = |\uparrow; \downarrow, \dots, \downarrow\rangle$ and

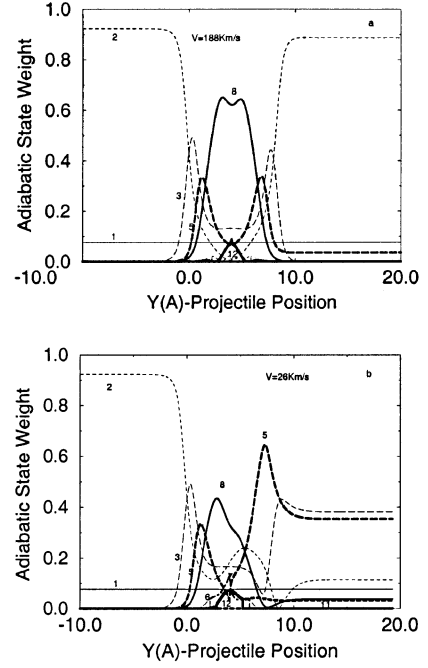


Fig. 5. The evolution of the weights of projected wavefunction $|\Phi\rangle$ on the adiabatic states for different projectile velocity with the condition of Figure 2.

the other $|b\rangle = \sum_{i \in M} (1/12^{1/2}) |\phi_i\rangle$, the sum is restricted to all 12 states $|\downarrow; \downarrow, \dots, \uparrow, \dots, \downarrow\rangle$ where the projectile is down and only one atom of the cluster is up. This choice shows that our initial state ($|\uparrow; \downarrow, \dots, \downarrow\rangle$) is the groundstate before the collision. But we could choose any combination of $|a\rangle$ and $|b\rangle$. During the collision the surface 1 is described by $|c\rangle = (|a\rangle + |b\rangle)/2^{1/2} = \sum (1/13^{1/2}) |\phi_i\rangle$.

The wavefunction $|\Phi\rangle$ could be expanded on the adiabatic surface states. The weight W_i of the different adiabatic states during the collision has been reported in Figure 5. For the adiabatic surface 1 we take during all the dynamics the state $|c\rangle$ and for the adiabatic surface 2 before the collision the state $|d\rangle = (12|a\rangle - |b\rangle)/145^{1/2}$. With such a choice our initial state has a projection on $|c\rangle$ and $|d\rangle$. During the process the state $|c\rangle$ is not coupled to the others and its weight remains constant. It is not the case for the state 2. The dynamics depends chiefly of the states 2, 3, 5 and 8 and weakly of the others 6, 10, 11 and 12. The coupling between states 2 and 3 begins at $Y \cong -2 \text{ \AA}$ (Fig. 4) leading to the decrease of the weight W_2 and the increase of W_3 . At $Y \cong -0.5(0.5) \text{ \AA}$ the coupling of the states 3-5 (5-8) begins leading to a maximum of W_3 (W_5). For $v_o = 1.88 \times 10^5 \text{ m/s}$ the weight evolution are looking nearly like even symmetry function with respect to the the axis $Y = 4 \text{ \AA}$. Note that at $Y = 4 \text{ \AA}$; $W_2 \cong 0$ and $W_8 \cong 0.6$; at the end of the process W_2 is slightly smaller than its initial value and only W_5 among the others is not zero. For $v_o = 0.26 \times 10^5 \text{ m/s}$ the evolution looks similar for $Y < 3 \text{ \AA}$, then it is more complex due to the interaction with state 6. The symmetry displays by the W_i disappears. At the end of the process nearly all the states have a weight different from zero. The contribution

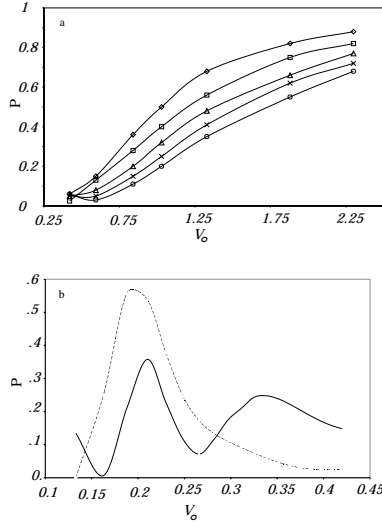


Fig. 6. Probability P that at the end of the diffusion process the projectile keeps its initial component *versus* the projectile velocity v_o ($\times 10^5$ m/s). (a) Study at high projectile velocity v_o for an impact parameter $b = 3.5$ Å and for a trajectory parallel to the C_n axis in the median plane of a face ($\diamond C_2$, $\square C_3$, $\triangle C_4$, $\times C_5$ and $\circ C_6$). (b) Study at low projectile velocity for a trajectory parallel to the C_2 axis in the median plane of a face and for an impact parameter $b = 4$ Å (dashed line) or $b = 3.5$ Å (solid line).

of the initial state in the adiabatic states 2, 3, 5 and 8 is respectively 0.41, 0.44, 0.044 and 0.018 for $Y \cong 0$ Å. It is explained why the projectile S_z is decreasing chiefly when the state 5 is activated in the first step of the dynamics. After the collision the cluster spin evolution is a combination of \sin or $\cos(\omega_n t)$ with $\omega_n = nJ/2\hbar$.

In Figure 6 we study the b variation of the probability P that at the end of the process the projectile keeps its up component for a median face trajectory. For v_o larger than 0.597×10^5 m/s, P exhibits a monotonous increase with b , the impact parameter. In Figure 6a, P is plotted for various b and for different C_n cluster size ($n = 2-6$) *versus* v_o (0.422×10^5 m/s $< v_o < 2.31 \times 10^5$ m/s). For a given C_n , P increases slowly at large v_o but at lower v_o where $\tau \cong \tau'$, there is a range where P varies rapidly. In this v_o -range, P goes to 0 for large n value. When v_o decreases (Fig. 6b), the P evolution with respect to v_o is strongly different and more random due to the fact that the projectile interacts with a full excited cluster. The dependence with the impact parameter is no more monotonous.

For projectile trajectories parallel to the C_n axis the depolarization cross-section D is given by:

$$D = \iint (1 - P(x, z)) dx dz \quad (5)$$

where P is the probability that the projectile keeps its initial spin component for a trajectory defined by x and z . For the 2D-integration we exclude trajectories which have an impact parameter smaller than 3 Å.

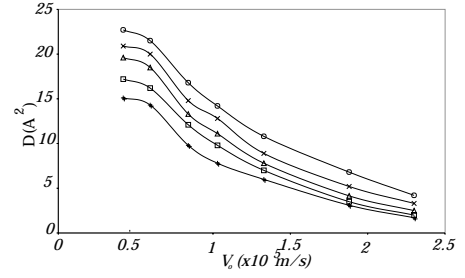


Fig. 7. Depolarization cross-section D (Å^2) *versus* the projectile velocity v_o for a trajectory parallel to the C_n axis ($\circ C_2$, $\times C_3$, $\square C_4$, $\triangle C_5$ and $+ C_6$) with an impact parameter $b = 3.5$ Å.

D has been studied *versus* v_o for different C_n (Fig. 7). D displays the same features as the ones described previously in Figure 2. Thus for 0.94×10^5 m/s $< v_o < 2.31 \times 10^5$ m/s, at given v_o , D is increasing with n but the difference between the C_n and C_{n+1} cross-sections is smaller when n increases. It is due to the fact that at every time that the projectile interacts with a target atom in this v_o -range the projectile atom becomes more and more down and it is less and less efficient in the diffusion process. Therefore at large v_o the cross-section reaches a geometric limit value when the cluster size increases. For 0.596×10^5 m/s $< v_o < 1.33 \times 10^5$ m/s the cross-section increases more, it is due to the fact that the projectile interacts longer with target atom. At $v_o = 0.422 \times 10^5$ m/s the cross-section D displays another behavior owing to the beginning of the collective phenomena in the target during the process.

4 Conclusion

The present article has shown the importance of the excitation of the cluster in the spin diffusion process. It would be interesting to investigate the excitation created by the diffusion in function of the cluster size, the impact parameter and the projectile velocity.

The authors thank the PROCOPE program for the financial help.

References

1. C. Bréchnac, Ph. Cahuzac, B. Concina, J. Leygnier, I. Tignères, Eur. Phys. J. D **12**, 185 (2000)
2. F. Martin, M.F. Politis, B. Zarour, P.A. Hervieux, Phys. Rev. A **60**, 4701 (1999)
3. R. Pfandzelter, T. Bernhard, H. Winter, Phys. Rev. Lett. **86**, 4152 (2001)
4. D. Oberli, R. Burgermeister, S. Riesen, W. Weber, Siegmann, Phys. Rev. Lett. **81**, 4228 (1998)
5. D. Maynaud, Ph. Durand, J.P. Daudey, J.P. Malrieu, Phys. Rev. A **28**, 3193 (1983)